Schenkel, J., Sekeris, C., Alonso, A., & Bautz, E. K. E. (1988) *J. Biochem. 171*, 565–569.
Swanson, M. S., & Dreyfuss, G. (1988a) *EMBO J. 7*, 3519–3529.
Swanson, M. S., & Dreyfuss, G. (1988b) *Mol. Cell. Biol. 8*, 2237–2241.
Wilk, H., Angeli, G., & Shafer, K. (1983) *Biochemistry 22*, 4592–4600.

Design of a Helix-Bundle Cross-Link: NMR and UV–Visible Spectroscopic Analyses and Molecular Modeling of Ring-Oxidized Retinals

Thomas C. Williams*,‡ and Venkatachalam Mani§

Departments of Pharmacology and Ophthalmology, Medical University of South Carolina, Charleston, South Carolina 29425-2251, and M&S Data Analysis and Molecular Speculations, Charleston, South Carolina 29417

Received July 19, 1990; Revised Manuscript Received December 17, 1990

ABSTRACT: In order to generate potential chemical cross-links for studying the chromophore binding site of bacteriorhodopsin and related helix-bundle proteins, MnO_2 was used to oxidize *all-trans*-retinal's ring moiety. The structures and solution conformations of three ring-oxidized retinal analogues have been determined by using UV–visible absorption and ^1H and ^{13}C NMR spectroscopies, primarily with regard to (i) the introduction of a functional group at the ring end of the chromophore, (ii) the retention of the all-trans geometry of the polyenal side chain, and (iii) the torsional angle of the ring–polyenal bond. Analyses of their UV–visible absorption spectral parameters (λ_{max}, ϵ_{max}, and vibrational fine structure) and NMR spectral parameters (^1H–^1H coupling constants, ^1H and ^{13}C NMR chemical shifts, and ^1H homonuclear Overhauser effects) indicated the 4-oxo and the 2,3-dehydro-4-oxo derivatives both possess the twisted 6-s-cis conformation adopted by most six-membered ring analogues of retinal in solution or crystal. However, the α-dioxocyclopentenyl analogue exists in solution predominantly (70–80%) as the planar 6-s-trans conformer, similar to violerythrine chromophore analogues. In order to identify the minor solution forms, molecular modeling and geometry optimizations using the semiempirical molecular orbital method AM1 defined two additional symmetry-related minima at ±30–40° in its C^6–C^7 torsional energy profile. Because the chromophores of bacterio- and halorhodopsins and sensory rhodopsins are bound as the 6-s-trans conformer [Harbison, G. S., Smith, S. O., Pardoen, J. A., Courtin, J. M. L., Lugtenburg, J., Herzfeld, J., Mathies, R. A., & Griffin, R. G. (1985) *Biochemistry 24*, 6955–6962; Baselt, D. R., Fodor, S. P. A., van der Steen, R., Lugtenburg, J., Bogomolni, R. A., & Mathies, R. A. (1989) *Biophys. J. 55*, 193–196], we suggest that the cyclopentenyl analogue's α-diketo function may be favorably positioned within the binding pocket and sufficiently reactive toward nucleophilic attack to cross-link an arginine located in or near the ring end of the chromophore cavity: Arg^{134} according to the current model of bacteriorhodopsin's tertiary structure [Henderson, R., Baldwin, J. M., Ceska, T. A., Zemlin, F., Beckmann, E., & Downing, K. H. (1990) *J. Mol. Biol. 213*, 899–929] or Arg^{82} as postulated from an alternate model constructed primarily to accommodate the external point charge contribution to bacteriorhodopsin's opsin shift [Spudich, J. L., McCain, D. A., Nakanishi, K., Okabe, M., Shimizu, N., Rodman, H., Honig, B., & Bogomolni, R. A. (1986) *Biophys. J. 49*, 479–483].

Probing the chromophore site of retinal-binding proteins has depended primarily upon studying the interactions of synthetic, conformationally well-characterized retinal analogues with proteins whose tertiary structures are essentially unknown (Balogh-Nair & Nakanishi, 1982; Crouch, 1986; Liu & Mirzadegan, 1988). The solution conformations of the major geometric isomers of retinal are described in the seminal works of Patel (1969), Honig et al. (1971), and Rowan et al. (1974); the crystalline structures for these and some related analogues are also known (Bart & MacGillavry, 1968; Gilardi et al., 1971; Schenk, 1971; Hamanaka et al., 1972; Gieren et al., 1982; Simmons et al., 1986a,b). However, for bacterial rhodopsins at least one of the conformational constraints that shapes the free chromophore in solution and in most crystalline lattices appears to be violated in the protein-bound chromophore. In retinals, the orientation of the ring relative to the polyenal chain is described by the C^5–C^6–C^7–C^8 torsional angle, ϕ^{5678}. In accord with calculated stabilities of the ring–chain conformers (Pullman et al., 1969; Honig et al., 1971), most unbound retinal chromophores exist in solution and crystal as twisted 6-s-cis forms where ϕ^{5678} is between −30° and −80°; protein-bound retinal analogues, however, can exist in the 6-s-trans form where ϕ^{5678} is assumed to be planar (i.e, 180°) as determined by analyses of ^{13}C NMR parameters in solid-state studies of bacteriorhodopsin (bR)[1] (Harbison et al., 1985) and by using the conformationally rigid 6-s-cis- and

* Author to whom correspondence should be addressed. Present address: M&S Data Analysis and Molecular Speculations, P.O. Box 30607, Charleston, SC 29417.
‡ Department of Pharmacology, Medical University of South Carolina.
§ Department of Ophthalmology, Medical University of South Carolina.

[1] Abbreviations: bR, bacteriorhodopsin; NMR, nuclear magnetic resonance; NOE, nuclear Overhauser effect; NOESY, two-dimensional NOE-correlated spectroscopy; COSY, two-dimensional *J*-correlated spectroscopy; AM1, Austin Method 1; $1^{(R,S)}$, prochiral designations of the geminal methyls at C^1 on the retinal ring.

0006-2960/91/0430-2976$02.50/0

6-s-trans-locked analogues in analyses of the opsin shift in bR (van der Steen et al., 1986) and halorhodopsins and sensory rhodopsins (Baselt et al., 1989).

An alternate approach to determining the three-dimensional structure of the chromophore site of retinal-binding proteins is via specific photoactivatable chemical modification of amino acid residues within the binding pocket (Balogh-Nair et al., 1981; Sen et al., 1982). Good candidates for such chemical modifiers should not only possess a reactive center distal to the normal Schiff base linkage but also be as sterically and electronically unperturbing as practicable. By using the *m*-diazirinophenyl and diazoacetoxy derivatives of retinal, such studies have tentatively identified residues within the chromophore binding site of bR, Ser^{193} and Glu^{194} being labeled by the former (Huang et al., 1982) and Thr^{121} and Gly^{122} by the latter (Ding et al., 1990). In order to evaluate the photoactivatable potential of carbonyl-containing retinal analogues, we synthesized 4-oxoretinal (Beischel et al., 1990). However, through serendipity rather than by design, we also isolated the α-dioxocyclopentenyl analogue of retinal, which, according to the current model of the tertiary structure of bR (Henderson et al., 1990), is potentially the simplest yet most specific cross-linker imaginable.

Henbest et al. (1957) have reported the manganese dioxide oxidation of the methylene group at C^4 in the cyclohexyl ring of retinal to form 4-oxoretinal. Weedon and co-workers have also determined that carotenoids partially oxidized at the ring undergo further oxidative ring contraction via a cyclic vicinal triketone intermediate to form α-dioxocyclopentenyl analogues (Holzel et al., 1969; Fatiadi, 1976, 1986). In this report, we discuss the identification and solution conformations of similarly oxidized retinals.

α-Dicarbonyl reagents are used routinely to modify a protein's arginyl residues exposed to the aqueous phase (Means & Feeney, 1971; Riordan, 1979; Gripon & Hofmann, 1981; Sleath et al., 1985). As applied to the opsin family of proteins, phenylglyoxal has been used to modify nine of the 12 arginine residues of native halorhodopsin, indicating that three of them probably lie within its transmembrane domain (Ariki et al., 1986). According to most current models of the bR, halorhodopsin, and sensory rhodopsin helix bundles, the three arginines unmodified by this reagent are most likely residue 4 on helix C, residue 2 on helix E, and residue 2 on helix F; that is, bR's Arg^{82}, Arg^{134}, and Arg^{175}, respectively. To account for the marked downfield ^{13}C NMR chemical shift of retinal-C^5 bR and yet normal ^{13}C chemical shift of retinal-C^7 bR, Harbison et al. (1985) postulated an ion pair near the β-ionone ring with its anionic component nearer C^5 and its cationic component—putatively arginine—nearer C^7. In accord with these observations and in order to account for the opsin shifts in a series of dihydro retinal analogues, the most recent version of the external point charge model of the retinal-binding site places an ion pair 3–4 Å above the face of the β-ionone ring (Honig et al., 1976; Nakanishi et al., 1980; Spudich et al., 1986). Because the α-dioxocyclopentenyl analogue of retinal cosely matches both the size and shape of the native chromophore and is potentially reactive toward cationic residues such as arginine or lysine, we suggest that it may serve to identify the positive point charge predicted by the models of Harbison et al. (1985) and Spudich et al. (1986).

Experimental Procedures

Synthesis of Oxoretinals. All-trans-retinal (Sigma; 100 mg, 0.35 mmol) in dry dichloromethane (15 mL) was stirred under dry nitrogen at 25 °C in the dark for 18 h with manganese dioxide (3 g) activated by heating at 180 °C for 1–2 h under house vacuum. The course of the reaction was monitored by using thin-layer chromatography (silica gel coated on plastic; ethyl acetate/hexane 35:65). Product mixtures were unaffected by either longer reaction times or additional manganese dioxide. The heterogeneous mixture was filtered through a Celite pad that had been washed previously with dichloromethane (25 mL). Solvent was removed under vacuum, and the products were isolated by chromatography on a silica column with gradient elution by ethyl acetate(0–50%)/hexane(100–50%). The reaction was also evaluated by using high-pressure liquid chromatography (250 × 4.6 mm Alltech Econosphere silica column) on a Varian 5000 instrument with a Waters 994 photodiode array detector. The products, referred to as oxoretinals **1**, **2**, and **3** (Chart I), were handled under dim red light and stored dry under argon at −70 °C.

Chart I

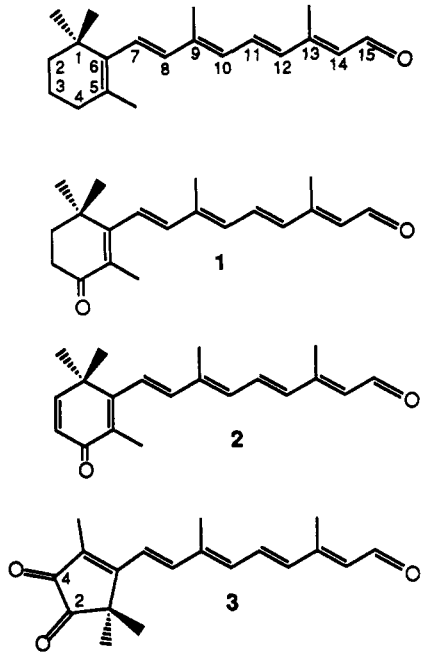

UV–Visible Absorption Spectroscopy. The isolated products were analyzed by using a Varian Cary 2200 spectrophotometer. The retinals were dissolved in ethanol or hexane, and spectra were recorded from 700 to 250 nm at room temperature. The molar absorptivity for the α-dioxocyclopentenyl analogue only was estimated from its ^1H NMR resonance intensities (in chloroform-*d*) and λ_{max} absorption intensity (in absolute ethanol) relative to 9-*cis*-retinal. For 9-*cis*-retinal, ϵ_{273} was taken as 36 100 L mol^{-1} cm^{-1} (Robeson et al., 1955).

IR Spectroscopy. The infrared absorption spectra of the isolated products were recorded on a Mattson Polaris FTIR spectrophotometer and analyzed with ICON software. Aliquots of the NMR samples in $CDCl_3$ (see below) were introduced into a NaCl sample cell (0.1-mm path length). After the sample compartment was purged with nitrogen gas, spectra were recorded from 4000 to 800 cm^{-1} at 1.0-cm^{-1} resolution.

Mass Spectrometry. The isolated products were analyzed by gas chromatography–mass spectrometry (GC–MS) on a Hewlett-Packard GC (5890)–MS (5970) instrument. Approximately 1 μg of the oxoretinals was injected into a fused silica capillary column at an initial temperature of 50 °C. The temperature was ramped at 20 °C min^{-1} to 290 °C. The effluent was ionized in the electron ionization mode, and the spectra were recorded from 50 to 350 m/z and analyzed for the molecular ions and characteristic retinal fragmentation products (e.g., $M^+ - 15$ and $M^+ - 43$).

^1H and ^{13}C NMR Spectroscopy. Data were collected and processed on a Varian VXR400 NMR spectrometer (Version 6.2b software) operating at 400 MHz for proton detection and 100 MHz for carbon. The oxoretinals were dissolved in $CDCl_3$ in the dark and examined in amberized tubes at 25 °C; once prepared, protection against isomerization by ambient fluorescent lighting was determined to be unnecessary.

Phase-sensitive two-dimensional homonuclear ^1H NMR data were acquired and processed by using the hypercomplex method (Bachmann et al., 1977; Mueller & Ernst, 1979, States et al., 1982) in order to produce pure phase absorption mode spectra. Scalar correlations were determined by using the double-quantum-filtered (2QF) version of the COSY pulse sequence (Aue et al., 1976; Piantini et al., 1982; Rance et al., 1983); nuclear Overhauser effect correlations were determined by using the NOESY pulse sequence (Jeener et al., 1979; Kumar et al., 1980; Macura et al., 1981). In order to optimize collection of 2QF-COSY data with high digital resolution, the spectral width in the ω_2 dimension was reduced to 700 Hz, sufficient to bracket the olefinic region only. A total of 512 1024-point free induction decays (FIDs) were collected and then Fourier transformed to a 2K × 2K data matrix to yield digital resolutions of 0.7 and 1.3 Hz for the ω_2 and ω_1 dimensions, respectively. Prior to the Fourier transformations, the t_2 domain FIDs and t_1 domain interferograms were multiplied by resolution enhancement and Lorentzian-to-Gaussian transformation functions with time constants of (acquisition time/2) for the former and 0.8(acquisition time/2) for the latter. NOESY spectra were acquired with a full spectral width of 5000 Hz in both dimensions and sufficient digitization to give resolutions of 2.5 and 4.9 Hz in ω_2 and ω_1, respectively. Separate data sets were collected in which the mixing time was varied (100, 200, or 500 ms) while allowing a sufficient relaxation delay to keep the recycle time constant at 2 s. The diagonal and cross peaks of the NOESY spectra were quantified by using the volume integration routine of the Varian software. ^1H chemical shifts were referenced to the residual $CHCl_3$ solvent resonance, taken as 7.27 ppm relative to tetramethylsilane (TMS).

Conventional NOE-enhanced proton-decoupled ^{13}C NMR spectra were obtained with a digital resolution of 1 Hz by using a spectral width of 30 000 Hz, a 60° observe pulse, an acquisition time of 0.5 s, and a 1.0-s relaxation delay; WALTZ-16 modulated broad-band decoupling (Shaka et al., 1983) was gated off during acquisition to obtain NOE-enhanced proton-coupled ^{13}C NMR spectra. ^{13}C chemical shifts were referenced to the center line of the solvent $CDCl_3$ triplet, taken as 77.0 ppm relative to TMS. The pulse sequence of Bax and Morris (1981) was used to collect one-bond and long-range ^1H–^{13}C heteronuclear chemical shift correlation spectra in the absolute value mode. For oxoretinals **1** and **2**, complete sets of one-bond ^1H–^{13}C NMR chemical shift correlations were collected in separate sets of two experiments: one in which only olefinic CH correlations were determined, the other in which only aliphatic CH correlations were determined. For the olefinic carbons, the spectral width was 1800 Hz in the δ_C dimension and 700 Hz in the δ_H dimension, yielding digital resolutions of 1.8 and 2.5 Hz, respectively. For the aliphatic carbons, the spectral width was 3000 Hz in the δ_C dimension and 700 Hz in the δ_H dimension, yielding digital resolutions of 1.5 and 2.5 Hz, respectively. A relaxation delay of 1.2 s was used for both data sets. Several long-range CH chemical shift correlations were also measured in order to assign unprotonated carbons by using a δ_C spectral width of 8400 Hz, a full-width δ_H of 5000 Hz, and a measured average long-range scalar interaction of approximately 5 Hz; the digital resolution was 4.4 Hz for δ_C and 10 Hz for δ_H. Because of the limited quantity of oxoretinal **3**, protonated carbon NMR assignments for the α-dioxocyclopentenyl analogue were determined by low-power, single-frequency, on-resonance decoupling; tentative assignments of the ipso carbon resonances were made on the basis of comparison to literature values of similar model compounds (see Results and Discussion).

Molecular Modeling. The oxoretinals were modeled by using Tripos' SYBYL program (Version 5.3) running on a DEC VAX 11/785 and manipulated on an Evans & Sutherland PS340 picture system. For the 4-oxo and 2,3-dehydro-4-oxo analogues, starting geometries were constructed by modifying the file of the crystal structure of *all-trans*-retinal (Hamanaka et al., 1972). For the α-dioxocyclopentenyl analogue, its initial geometry was approximated as a hybrid of the C^7–C^{15} polyenal portion of *all-trans*-retinal and the trimethyldioxocyclopentenyl portion of the violerythrine chromophore analogues determined crystallographically by Martin et al. (1987).

Molecular geometries were optimized by using the AM1 semiempirical molecular orbital calculations program of Dewar et al. (1985) as implemented by SYBYL's Quantum Chemistry Program Exchange options. For the α-dioxocyclopentenyl analogue only, *quasiglobal* minimum-energy geometries were calculated as a function of the ϕ^{5678} torsional angle. During each *pseudoadiabatic* geometry optimization, all bond lengths, all bond valence angles, and all methyl rotor dihedrals were allowed to vary; however, all other torsional angles were held constant, the atoms in the polyenal portion restricted to one plane and the atoms of the dioxocyclopentenyl ring to another. The ϕ^{5678} torsional angle was varied by 10° increments from 0° (planar 6-s-cis) to 180° (planar 6-s-trans); at each increment, the geometry was reoptimized at selected combinations of methyl group rotations (15–30° increments) in order both to determine the *quasiglobal* minimum-energy geometry at the selected ϕ^{5678} and to estimate the torsional barriers for rotation of 1^RCH_3, 1^SCH_3, $5CH_3$, and $9CH_3$. Because semiempirical methods underestimate significantly the torsional barrier of single bonds in conjugated systems, the torsional barrier for the C^6–C^7 bond of the desmethyl α-dioxocyclopentenyl analogue truncated at C^{10} was also calculated by optimizing its geometry as a function of ϕ^{5678}. By determining AM1's estimate of this barrier, an appropriate correction to the cis → trans barrier height was calculated from comparison to experimental determinations for the rotational barrier of the central bond of 1,3-butadiene, which range from 3.9 to 4.7 kcal mol^{-1} (Bock et al., 1979; Squillacote et al., 1979).

Results and Discussion

Chromophore Structure Determinations. Data for the initial characterization of three products (oxoretinals **1**, **2**, and **3**; Chart I) isolated from manganese dioxide oxidation of *all-trans*-retinal are summarized in Table I. From their UV–visible absorption spectra obtained in ethanol, these products were determined to be "retinallike", each having intense $\pi\pi^*$ absorption as evidenced by the $^1B_u^+ \leftarrow {}^1A_g^-$ band at $\lambda_{max} \geq 350$ nm expected for enal chromophores with extended conjugation (Honig et al., 1980). For example, in ethanol the λ_{max} for oxoretinal **3** was 435 nm and its ϵ_{max} was 45 000 ± 5000 L mol^{-1} cm^{-1}. Furthermore, each oxidation product showed intense absorption(s) in its IR spectrum at frequencies between 1700 and 1650 cm^{-1}, indicating the presence of carbonyl function(s) other than the conjugated aldehyde as determined by comparison with the IR spectrum of *all-trans*-retinal.

Table I: Spectroscopic Characterization of MnO_2-Oxidized Retinals

	λ_{obs}[a] (nm)	λ_{calc}[b] (nm)	m/z[c]	$\nu_{C=O,s}$[d] (cm^{-1})	$\nu_{C=O,a}$[d] (cm^{-1})
locked 6-s-trans[e]	400	437			
locked 6-s-cis[e]	414	412			
all-trans-retinal	378	414	284		
oxoretinal **1**	378	444	298	1654	
oxoretinal **2**	380	444	296	1654	
oxoretinal **3**[f]	435	434	298	1654	1690
model dioxo[g]				1690	1755

[a] Observed wavelength (in ethanol) of the maximum absorption of the $^1B_{u^+} \leftarrow {}^1A_{g^-}$ band. [b] Calculated according to Woodward's rules (1941, 1942a,b) as modified by Fieser and Fieser (1959), Scott (1964), and Pasto and Johnson (1969). [c] Mass-to-charge ratio of parent ion. [d] Ketone carbonyl stretching frequency; in the case of the dioxo function, s = symmetric mode and a = asymmetric mode. [e] Observed λ_{max} taken from van der Steen et al. (1986). [f] $\epsilon_{435} = 45\,000 \pm 5000$ L mol^{-1} cm^{-1}. [g] From Martin et al. (1987) for 3,5,5-trimethyl-4-vinylcyclopent-3-ene-1,2-dione.

The structure of the polyenal side chain of each of these oxidation products was determined by analysis of its ^1H NMR spectrum. Because of the marked segregation of resonance groups in the ^1H NMR spectrum of retinal, high-resolution two-dimensional correlated spectra were measured readily with significant reductions in both the data table size and acquisition time by centering the transmitter frequency in the olefinic region and then reducing the spectral width to one-seventh that normally required. Correlations to folded-over frequencies were easily detected and identified; scalar spin–spin interactions between methyl protons and olefinic protons up to eight bonds distant along the polyene chain were observed clearly as correlations unsymmetrical about the diagonal. Each analogue showed a doublet resonance at about 10.1 ppm characteristic of the aldehyde proton at C^{15}, each showed four singletlike resonances in a 1:1:1:2 integration ratio between 2.5 and 1 ppm, confirming the presence of the five methyls of normal retinals, and each showed several multiplet resonances in the olefinic region characteristic of retinal's conjugated polyenal system (Table II). From two-dimensional *J*-correlated spectroscopy, all ^1H NMR resonances were assigned readily by analyzing their vicinal and long-range scalar ^1H–^1H interactions (Figure 1, left side of panels). Chemical shifts were calculated from the line positions of the multiplet resonances, with second-order effects taken into account. Coupling constants were measured directly from observed splittings in resolution-enhanced one-dimensional spectra or estimated from the peak separations of the antiphase multiplets in the ω_2 dimension of the 2QF-COSY spectra. Long-range proton–proton couplings not resolved in one-dimensional spectra were clearly detected by 2D spectroscopy. Most evident were the interactions involving the folded-over methyl resonances. For example, the $^4J_{10,9CH_3}$ and $^5J_{7,5CH_3}$ scalar interactions produced cross peaks nearly as intense as those derived from the vicinal interactions between olefinic protons whereas $^4J_{12,14}$ and $^5J_{11,14}$ were detectable in contour plots only at a very low relative threshold level. For these long-range correlations, however, measurements of the peak separations in cross peaks with unresolved fine structure yielded estimates that were nearly twice the value of the active coupling (as measured directly from observed splittings in the one-dimensional spectra) if the coupling was second largest for a given resonance or 4 times or more if it was third or less in relative value. These approximate correction factors were invoked primarily on the assumption that the inner portions of the cross peaks' fine structure canceled to zero intensity due to the antiphase nature of the active coupling and its approximate magnitude relative to additional passive couplings within the same cross peak.

Table II: ^1H NMR Chemical Shifts and Coupling Constants for Oxoretinals[a]

proton	oxo **1**	oxo **2**[b]	oxo **3**[b]
		δ	
$1,1'CH_3$	1.19	1.29 (0.10)	1.43 (0.24)
2H	1.86	6.79	
3H	2.51	6.25	
$5CH_3$	1.85	2.02 (0.17)	2.10 (0.25)
7H	6.37	6.44 (0.07)	6.70 (0.33)
8H	6.34	6.48 (0.14)	7.15 (0.81)
$9CH_3$	2.06	2.10 (0.04)	2.14 (0.08)
10H	6.29	6.34 (0.05)	6.57 (0.28)
11H	7.12	7.14 (0.02)	7.15 (0.03)
12H	6.44	6.47 (0.03)	6.59 (0.15)
$13CH_3$	2.34	2.35 (0.01)	2.37 (0.03)
14H	5.99	6.02 (0.03)	6.06 (0.07)
15H	10.12	10.14 (0.02)	10.16 (0.04)
		^3J	
7,8	16.3	16.2	16.2
10,11	11.4	11.5	11.6
11,12	15.1	15.1	15.1
14,15	8.1	8.0	7.9
		$>^3J$	
8,10		0.56	
10,12	[c]	[c]	[c]
11,14	<0.8	0.6	0.5
12,14	[c]	[c]	[c]
$5CH_3,3$		[c]	
$5CH_3,7$	0.84	0.75	0
$9CH_3,10$	1.18	1.22	1.19
$9CH_3,11$	[c]	[c]	[c]
$9CH_3,12$	[c]	[c]	[c]
$9CH_3,14$	[c]	[c]	[c]
$13CH_3,14$	1.15	1.13	1.19

[a] All shifts in ppm ±0.01; all coupling constants in Hz ±0.1 unless indicated otherwise. [b] Parentheses indicate chemical shift differences relative to oxoretinal **1**. [c] Detected by 2QF-COSY but not quantified due to peak cancellation effects (see text; estimated to be <0.5 Hz).

With few exceptions (see Chromophore Conformational Analyses, below), the ^1H resonance assignments and coupling constants were consistent with literature values for the polyenal portion of all-trans isomers of retinal and its analogues (Patel, 1969; Rowan et al., 1974; Wernly & Lauterwein, 1983). Because each of these three oxidized products possessed the unmodified tetraenal chain characteristic of retinals, we concluded that their structural differences were restricted entirely to the ring portion.

In the ^1H NMR spectrum of oxoretinal **1**, the only resonances left unassigned following analysis of the polyenal chain were two tripletlike multiplets in the aliphatic region, one at 2.51 ppm and the other at 1.86 ppm. Because the latter showed a significant NOE with the $1,1'CH_3$ resonance, it was assigned to methylene protons at C^2; the former showed both scalar and NOE correlations to the C^2 methylene protons and was assigned to methylene protons at C^3. Because the chemical shift of the C^3H_2 resonance was characteristic of protons α to a carbonyl function, oxoretinal **1** was therefore identified as 4-oxoretinal, in agreement with the mass and IR spectral data presented in Table I and ^1H NMR assignments made in a previous analysis (Sokolova et al., 1979). Oxoretinal **2**, having no aliphatic ^1H resonances other than those assigned to the methyls but showing two additional olefinic doublets characteristic of an isolated –CH=CH– moiety, was tentatively identified as 2,3-dehydro-4-oxoretinal. Because oxoretinal **3** had no ^1H resonances left unassigned after analysis of its polyenal portion, its ring was, therefore, presumably aprotic. Consistent with both its IR and mass spectral data, oxoretinal **3** was identified tentatively as the α-dioxocyclopentenyl analogue of retinal.

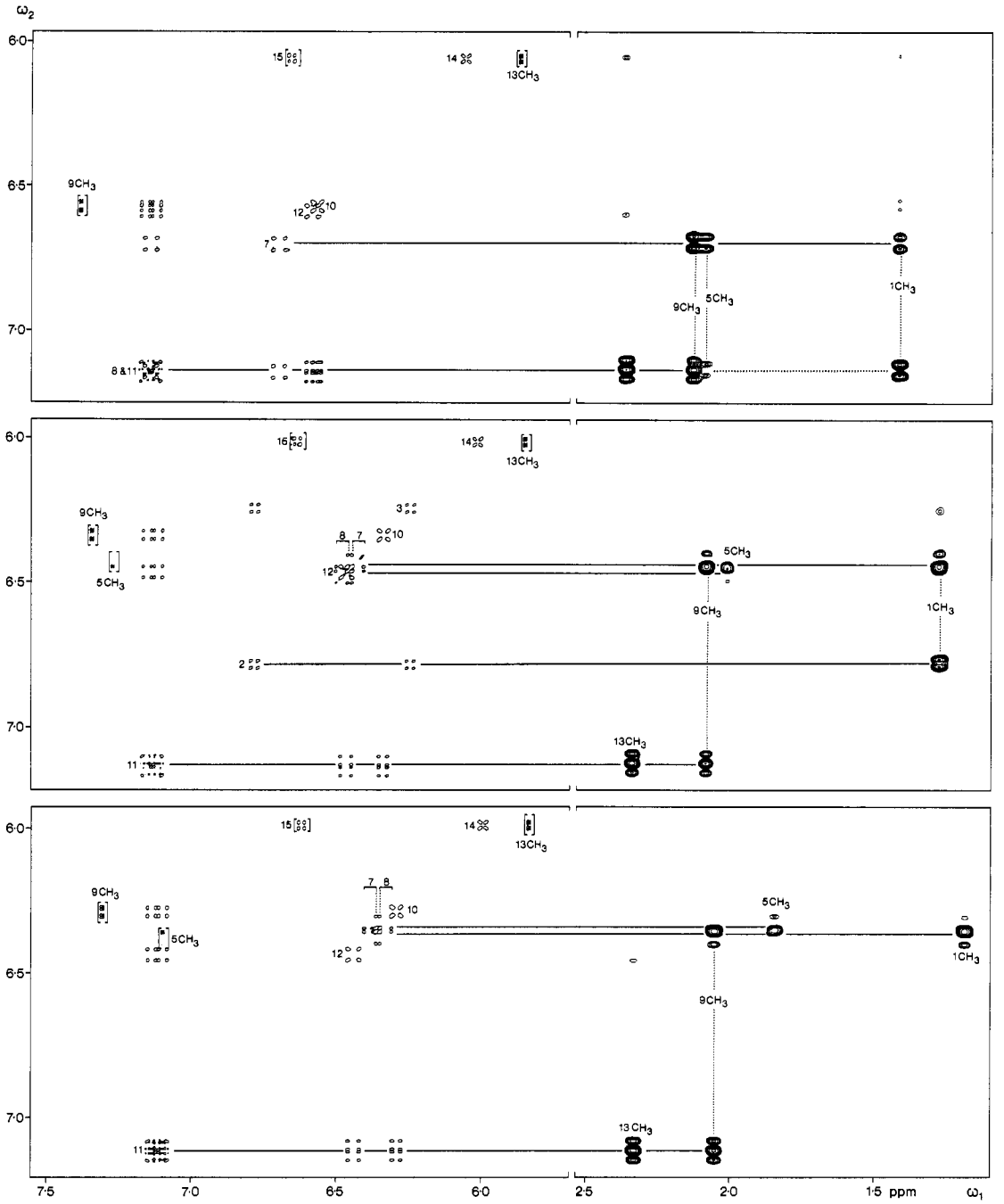

FIGURE 1: Two-dimensional homonuclear 400-MHz ^{1}H NMR spectra of oxoretinals (10 mM, $CDCl_3$, 25 °C). Bottom panel, 4-oxoretinal; middle panel, 2,3-dehydro-4-oxoretinal; top panel, α-dioxocyclopentenylretinal. The left portion of each panel shows the reduced spectral width 2QF-COSY of the olefinic region with asymmetric cross peaks generated by fold-over correlations bracketed; the right portion of each panel shows the appropriate off-diagonal expansion from the 500-ms NOESY spectrum for each oxoretinal. Solid horizontal lines highlight the NOE correlations between olefinic and methyl group protons; the dotted vertical lines join the multiple NOEs made by a single methyl group to different olefinic protons.

The ring structure of these oxidized retinals were confirmed by analyzing their ^{13}C NMR spectra. For *all-trans*-retinal, three of the six carbons in its unmodified trimethyl cyclohexenyl ring (i.e., C^1, C^5, and C^6) appear normally as weak resonances due primarily to the relaxation differential and heteronuclear NOE favoring protonated carbons (Rowan & Sykes, 1974; Becker et al., 1974). For oxoretinal **1**, however, four of the six carbons not assigned to its polyenal portion appeared with weak intensity in its ^{1}H-decoupled ^{13}C NMR spectrum, indicating that they were nonprotonated. The chemical shifts of two of these four nonprotonated ring carbon resonances matched closely those expected for C^1 and C^5; because the resonances at 37.35 and 34.24 ppm had been assigned to the two protonated ring carbons at C^2 and C^3, respectively, on the basis of their two- and three-bond scalar C–H couplings (Table III), the resonance at 199.15 ppm (Figure 2) was assigned to C^4, a carbonyl carbon, and that at 160.54 ppm to C^6, β to an α,β-unsaturated carbonyl (not shown), thereby confirming the identification of oxoretinal **1** as 4-oxoretinal. For oxoretinal **2**, two additional ^{13}C NMR resonances were detected in the olefinic region and two fewer were observed in the aliphatic. The resonance at 156.72 ppm was assigned to C^2, β to the carbonyl at C^4, and the resonance at 125.96 ppm was assigned to C^3, thereby confirming the identification of oxoretinal **2** as 2,3-dehydro-4-oxoretinal. By comparison to the spectrum of 4-oxoretinal, the ^{13}C NMR spectrum of oxoretinal **3** showed several differences (Figure 2): an additional carbonyl resonance, the disappearance of

Table III: ^{13}C NMR Chemical Shifts of Oxoretinals Compared to Those of Model Compounds

carbon	*all-trans*-retinal[a]	oxoretinal[b] oxo 1	oxo 2	oxo 3	model α-cyclopentenedione[c]
1	34.6	35.70	*d*	44.34	44.3
2	40.0	37.35	156.72	203.60	203.2
3	19.5	34.24	125.96		
4	33.4	199.15	189.90	188.12	188.7
5	130.3	130.31	130.53	141.03	140.4
6	138.2	160.54	157.30	167.85	168.0
7	129.2	126.81	125.96	121.33	128.7
8	137.8	140.19	140.96	145.72	128.0
9	140.5	139.45	139.35	139.30	
10	130.3	132.47	132.87	137.90	
11	132.1	131.61	131.53	130.96	
12	135.6	136.50	136.76	139.52	
13	153.6	154.04	153.98	153.17	
14	129.7	129.77	129.90	130.87	
15	190.4	191.06	191.10	191.02	
1,1′CH_3	29.0	27.59	27.08	23.07	22.6
5CH_3	21.6	13.74	13.49	9.41	9.1
9CH_3	12.5	12.86	12.90	12.61	
13CH_3	12.5	13.10	13.13	13.11	

[a] From Becker et al. (1974) as ppm relative to TMS in dioxane. [b] This work, as ppm (±0.05) relative to TMS in $CDCl_3$ at 25 °C. [c] From Martin et al. (1987) for 3,5,5-trimethyl-4-vinylcyclopent-3-ene-1,2-dione as ppm relative to TMS in $CDCl_3$ at 25 °C. [d] Not determined due to the presence of minor impurities.

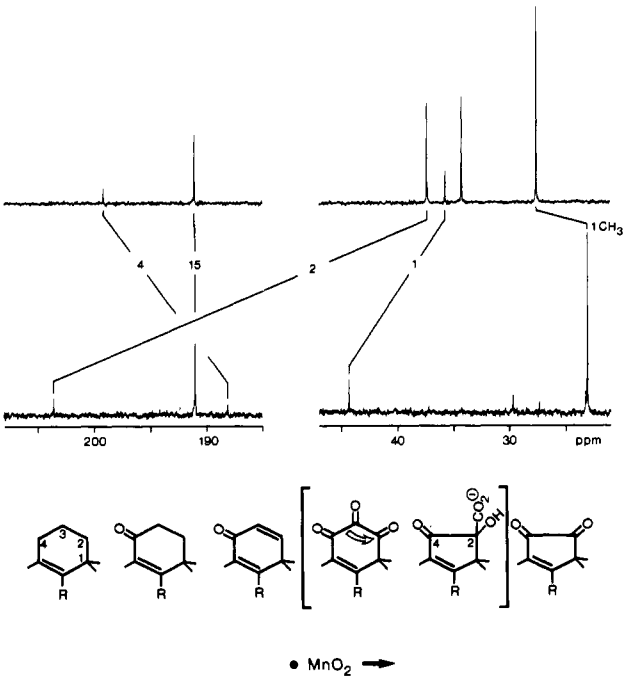

FIGURE 2: Ring contraction of oxoretinal **3**. Top panel, comparison of the ^1H-decoupled 100-MHz ^{13}C NMR spectra of 4-oxoretinal (upper trace) and α-dioxocyclopentenylretinal (lower trace); highlighted by line correlations between these spectra are (i) the conversion of C^2 from a methylene carbon to a carbonyl carbon, (ii) the retention of the C^4 carbonyl and quaternary C^1 carbons, and (iii) the loss of the C^3 methylene carbon. Bottom panel, scheme of the MnO_2 oxidation of retinal's β-ionone ring [after Holzel et al. (1969) and Kollenz and Akcamur (1984)].

the C^2 and C^3 resonances, and the retention of the C^1, C^4, C^5, and C^6 resonances. The conversion of one methylene carbon to a carbonyl with the net loss of one carbon indicated that the ring was five-membered with α-diketo substitution, thereby confirming the identification of oxoretinal **3** as the dioxocyclopentenyl analogue. The MnO_2-mediated oxidation of the ionone ring of retinal that presumably led to the formation of oxoretinals **1**, **2**, and **3** is summarized by the scheme in Figure 2 (Holzel et al., 1969; Kollenz & Akcamur, 1984).

Chromophore Conformation Analyses. As indicated in Table I, λ_{max} for α-dioxocyclopentenylretinal calculated according to the empirical relationships of Woodward's rules (Woodward, 1941, 1942a,b; Allinger & Tai, 1965) is nearly identical with its observed λ_{max}; however, the correspondence between calculated and observed λ_{max} values for retinal, 4-oxoretinal, and 2,3-dehydro-4-oxoretinal is poor. This discrepancy between calculated and observed λ_{max} values for retinals is ordinarily attributed in only a qualitative sense to the twist of the C^6–C^7 single bond. One can, however, use this discrepancy to estimate ϕ^{5678} quantitatively (Honig et al., 1975, 1976). If one assumes that the π system within the ring portion of retinal analogues could be completely uncoupled from the polyenal side chain by twisting the C^6–C^7 bond 90° in order to orient the ring perpendicular to the plane of the side chain, then the calculated λ_{max} would be 355 nm—a difference of 59 nm compared to the calculated λ_{max} for the extended, fully coplanar chromophore. If one assumed further that the observed λ_{max} was approximated as a linear function of ϕ^{5678}, the time- or population-weighted average twist about the C^6–C^7 single bond could then be estimated for *all-trans*-retinal as one of four λ_{max}-indistinguishable orientations, ±55° or ±125°. Likewise, for 4-oxoretinal and 2,3-dehydro-4-oxoretinal, the ±65° and ±115° orientations would be predicted from the observed λ_{max} of these analogues. Of these four orientations, only the symmetry-related pair with $|40|° < \phi^{5678} < |70|°$ is consistent with their NOE-determined orientations (see below). For α-dioxocyclopentenylretinal, the near equivalence of its calculated and observed λ_{max} values indicated that all portions of the polyenalone system are coplanar, ϕ^{5678} being 0° or 180°. For this analogue, only the $\phi^{5678} = 180°$ torsional angle was consistent with the NOE-determined predominant orientation described below.

These λ_{max}-based evaluations of ϕ^{5678} in the oxoretinals are further supported by similar comparisons of λ_{obs} and λ_{calc} for the 6-s locked analogues of *all-trans*-retinal (van der Steen et al., 1986; Baselt et al., 1989). *All-trans*-retinal covalently locked in the 6-s-trans conformation by a methylene bridge between one of the methyls at C^1 and C^8 is predicted by Woodward's rules to have a $\lambda_{calc} = 437$ nm if the chromophore is fully coplanar (Table I). However, its 37-nm deficit indicates that the C^6–C^7 bond is twisted by about |40|°. Molecular modeling indicates that the cyclohexenelike locking ring formed by the bridge between $1CH_3$ and C^8 twists C^6–C^7 |20–40|° out-of-plane, in good agreement with experiment. Similarly, *all-trans*-retinal covalently locked in the 6-s-cis conformation is predicted to have a $\lambda_{calc} \approx 412$ nm. Such a bridge forces the locking ring to assume a planar conformation, the agreement between λ_{obs} and λ_{calc} being excellent (414 vs 412 nm).

In addition to its λ_{max}, the appearance of resolved vibrational fine structure within the $^1B_u^+ \leftarrow {}^1A_g^-$ band of the UV–vis spectrum of α-dioxocyclopentenylretinal indicated that the conformation of its ring–chain juncture is well-defined (Figure 3). Retinal isomers and analogues whose ϕ^{5678} torsional energy minimum is relatively broad show a diffuse $^1B_u^+ \leftarrow {}^1A_g^-$ band in either ethanol or hexane solution (Honig et al., 1980), the C=C stretching progression characteristic of polyenes being obscured by the sensitivity of this band's λ_{max} to the C^6–C^7 torsional angle (Warshel & Karplus, 1974). Compared to the calculated stretching progression for β-ionone and retinals (≈1620 cm^{-1}), the stretching progression for the dioxo analogue was lower (1430 cm^{-1}), consistent qualitatively with the addition of the conjugated ring carbonyl. In order

Table IV: Relative NOEs and Calculated Interproton Distances for α-Dioxocyclopentenylretinal

correlation	NOE_{rel}[a]			internuclear distances[b]			
	τ_m = 100 ms	τ_m = 200 ms	τ_m = 500 ms	r_{app}	r_{180}	r_0	r_{mix}
[7H,1,1′CH_3]	0.437	0.487	0.498	3.6	4.45	2.98	3.6
[7H,5CH_3]	0.602	0.545	0.570	3.1	2.82	4.65	3.0
[7H,9CH_3]	1.365	1.275	1.383	2.7	2.72	2.72	
[8H,1,1′CH_3]	1.513	1.514	1.165	3.0	2.90	5.18	3.0
[8H,5CH_3]	0.050	0.099	0.198	3.7	5.39	2.63	3.5
[8H,9CH_3]	c	c	c	c	3.88	3.87	
[11H,9CH_3]	1.025	1.152	1.065	2.8	2.76	2.76	
[11H,13CH_3]	1.144	1.181	1.151	2.8	2.76	2.76	
[12H,14H]	1.000	1.000	1.000	2.35	2.35	2.35	
[15H,13CH_3]	(0.66)	0.693	0.695	3.0	2.86	2.86	

[a] Integrated cross-peak volumes relative to the [12H,14H] NOESY correlation as a function of mixing time (τ_m); $r_{12,14}$ taken as 2.35 Å (Hamanaka et al., 1972; AM1 results, this work). [b] r_{app} (±0.1 Å) calculated based on $r_{12,14}$ = 2.35 Å; r_{180} and r_0 taken as the geometry-optimized internuclear distances for the 6-s-trans and 6-s-cis conformers corrected for the dynamic displacement of the methyl centroids due to methyl rotation; r_{mix} calculated from the weighted average of NOEs for a mixture of conformers (70–80% r_{180}/10–15% $r_{+(30-40)}$/10–15% $r_{-(30-40)}$). [c] The [8H,9CH_3] interaction showed no significant NOE as judged by the fine structure of the [11H,9CH3] cross peak (see text).

to observe vibrational fine structure within the main ππ* band, the number of energetically allowed conformations that permit any degree of conjugation between chain and ring must be reduced. For instance, in anhydroretinal the main absorption band is characterized clearly by vibrational fine structure, the ring and chain being forced into one coplanar conformation by the exocyclic C^6=C^7 double bond (Honig et al., 1980). Alternatively, the π-system in any unsaturated ring could be effectively uncoupled from the π-system of the polyene chain by changing the hybridization of C^6 from sp^2 to sp^3; α-retinals, for example, exhibit vibrational fine structure in their main absorption band, due primarily to the *insensitivity* of its λ_{max} toward the C^6–C^7 torsional angle (Asato et al., 1989).

The NOESY correlations served both to confirm the all-trans geometry of the polyenal side chain of all three oxo-retinals and to assess the torsional angle of the ring–chain juncture in each analogue. In combination with measurements of vicinal and long-range scalar couplings along the polyenal chain, observation of four strong NOEs between the following olefinic protons and allylic methyls indicated that the polyenal chain was all-trans in each oxo derivative (Figure 1, right side of panels): [7H,9CH_3], [11H,9CH_3], [11H,13CH_3], and [15H,13CH_3].

For 4-oxoretinal and 2,3-dehydro-4-oxoretinal, the torsional angle ϕ^{5678} was evaluated qualitatively by comparing the integrated cross-peak volume of the [7H,1,1′CH_3] dipolar interaction to that of [8H,5CH_3], the [7H,5CH_3] and [8H,1,1′CH_3] NOESY correlations being too weak to detect. Because 7H and 8H are tightly coupled in both of these retinal analogues, accurate measurement of these NOEs was difficult and quantitative interpretation unwarranted; however, the marked preference for NOEs between [7H,1,1′CH_3] and [8H,5CH_3] is qualitatively consistent with the twisted 6-s-cis geometry found for most β-ionone-ring-containing retinal analogues in the solid state and all in solution. For these two analogues, ϕ^{5678} was therefore assumed to be between −40 and −70° (Honig et al., 1971).

In the α-dioxocyclopentenyl analogue, 7H and 8H are loosely coupled, resulting in four well-resolved NOE cross peaks that could be integrated readily in an attempt to quantitate the torsional angle ϕ^{5678}. Table IV summarizes the NOE correlations for this analogue measured at 100-, 200-, and 500-ms mixing times. For each of these three experiments, the NOE intensities were normalized relative to the integrated volume of the [12H,14H] cross peak. Making the appropriate assumptions concerning the relaxation behavior of protons in retinals (Honig et al., 1971) and further assuming that the [12H,14H] interproton distance is independent of ϕ^{5678} and

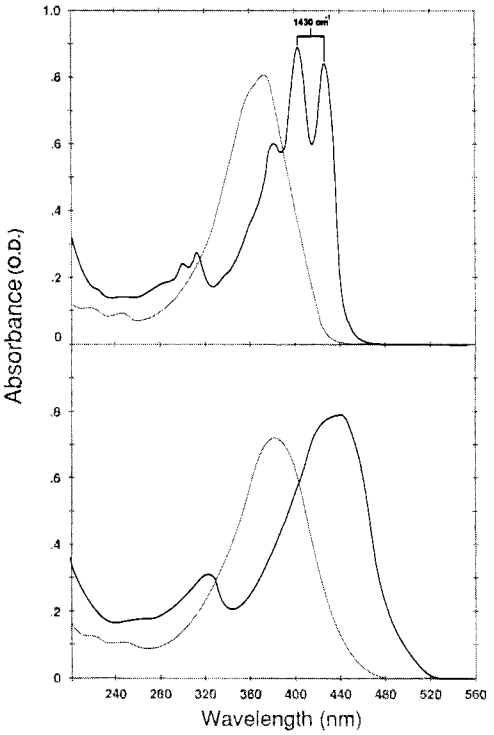

FIGURE 3: UV–visible absorption spectra of α-dioxocyclopentenyl-retinal (black line) and *all-trans*-retinal (gray line) in absolute ethanol (bottom panel) and hexane (top panel). The C=C stretching progression (1430 cm^{-1}) evidenced by the vibrational fine structure in the spectrum of the α-dioxo analogue in hexane is indicated.

fixed at 2.35 Å (Hamanaka et al., 1972; AM1 molecular geometry optimization results, this work), we have calculated from these observed NOEs the apparent absolute interproton distances necessary for determining the torsional angle ϕ^{5678}. Over the range chosen, all but one of the calculated interproton distances appeared to be independent of the mixing time used to measure the NOE correlation. The [8H,5CH_3] correlation, however, did not show this independence; as the mixing time increased, the apparent $r_{8,5CH_3}$ decreased. This we attribute to the inaccuracies in measuring cross-peak volumes of weak correlations at relatively short mixing times. That 8H did not appear to be dipolar-coupled to 9CH_3 was attributed to the acute geometry of the pseudo-three-spin 9CH_3–7H–8H system (Noggle & Schirmer, 1971). Some of the internuclear distances calculated from those relative experimental NOEs dependent on ϕ^{5678} are in fair agreement with those predicted from the methyl centroid model (Rowan et al., 1974) of the

AM1 geometry-optimized structure of the 6-s-trans conformer (Table IV). However, the discrepancies observed indicated that the sample was a mixture of conformers. In order to evaluate these discrepancies, the potential energy profile for the torsion about the C^6–C^7 bond was determined by plotting the heat of formation output from the AM1 calculations as a function of ϕ^{5678}. The *static* quasiglobal minimum energy profile (Figure 4, bottom) indicated that the twisted (±20°) 6-s-cis conformers were favored by 1.3 kcal mol^{-1}. However, if one adds to this profile the methyl rotation barriers calculated as a function of ϕ^{5678} (Figure 4, top; Figure 5, far right), the resultant profile indicated that three conformers of near equal stability should coexist—two twisted (±40°) 6-s-cis and one planar 6-s-trans (Figure 4, bottom panel, uppermost profile). Correcting this *dynamic* quasiglobal minimum energy profile for the inherent AM1 underestimate of the single-bond torsional barrier in conjugated systems (2.3 kcal mol^{-1}; Figure 4, middle) yielded a profile that predicts the planar 6-s-trans conformer to be favored by about 0.7–0.9 kcal mol^{-1} over two twisted (±30–40°) 6-s-cis conformers (Figure 4, bottom panel, shaded profiles). Relative NOEs for these geometry-optimized conformers were calculated and weighted average NOEs determined in order to compare to the observed NOEs of the mixture. As shown in Table IV, all of the internuclear distances calculated from the observed NOEs matched those predicted for a mixture of 6-s-trans (70–80%) and twisted (±30–40°) 6-s-cis (10–15% each) conformers (Figure 5). In order to achieve such a mixture, the energy difference between the trans and twisted cis conformers should be between 0.9 and 1.1 kcal mol^{-1}; this indicates that the inherent torsional barrier about the C^6–C^7 single bond in the conjugated system of retinals is about 5.5 kcal mol^{-1} rather than the 3.9–4.7 kcal mol^{-1} range estimated from experimental determinations for the torsional barrier of the central single bond in butadiene (Bock et al., 1979; Squillacote et al., 1979). This is not unreasonable in view of the 7.4–8.9 kcal mol^{-1} barrier determined for the central single bond in acrolein and related compounds by ab initio molecular orbital calculations (Loncharich et al., 1987).

Two additional lines of evidence support the NOE-determined predominantly planar 6-s-trans geometry of α-dioxocyclopentenylretinal. First, the homoallylic five-bond coupling between 7H and $5CH_3$ is nonzero for nonplanar ϕ^{5678} torsional angles; in retinals and the 4-oxo and 2,3-dehydro-4-oxo analogues studied here, this coupling is between 0.75 and 0.90 Hz, indicating that ϕ^{5678} is twisted about 30° out-of-plane (Karplus, 1960; Barfield & Chakrabarti, 1969; Honig et al., 1971). For the α-dioxocyclopentenyl analogue, however, $^5J_{7,5CH_3}$ is zero (Table II), indicating that ϕ^{5678} is either 0° or 180°. Second, the ^1H NMR chemical shifts of $1,1'CH_3$, 7H, 8H, $5CH_3$, and 10H are significantly deshielded relative to retinal analogues with twisted 6-s-cis geometry (Table II). This can be interpreted as steric interactions between these methyl protons and 7H, 8H, and 10H similar to the steric deshielding of the 11H resonance by the [11H,$9CH_3$] and [11H,$13CH_3$] interactions, most severe when the analogue is restricted to planar 6-s-cis geometry (Cheney, 1968; Patel, 1969; Honig et al., 1971; Rowan et al., 1974). Analogous to these deshielded ^1H NMR resonances are the shielded ^{13}C NMR resonances of $1,1'CH_3$, $5CH_3$, and 7H (Table III), shifted upfield due to the same sterically induced C–H bond polarizations that shifted the ^1H NMR resonances downfield (Cheney & Grant, 1967; Grant & Cheney, 1967; Cheney, 1968; Rowan & Sykes, 1974).

Modeling the Cross-Link Connection. Intensive computer modeling guided by many biophysically and biochemically determined constraints has allowed Henderson et al. (1990) to interpret their electron diffraction data of purple membrane in terms of a detailed three-dimensional structure of bR having effective Fourier resolutions of 3.5 Å parallel and 10 Å perpendicular to the membrane plane. Key to this model's construction was the assignment of helices A and B to positions

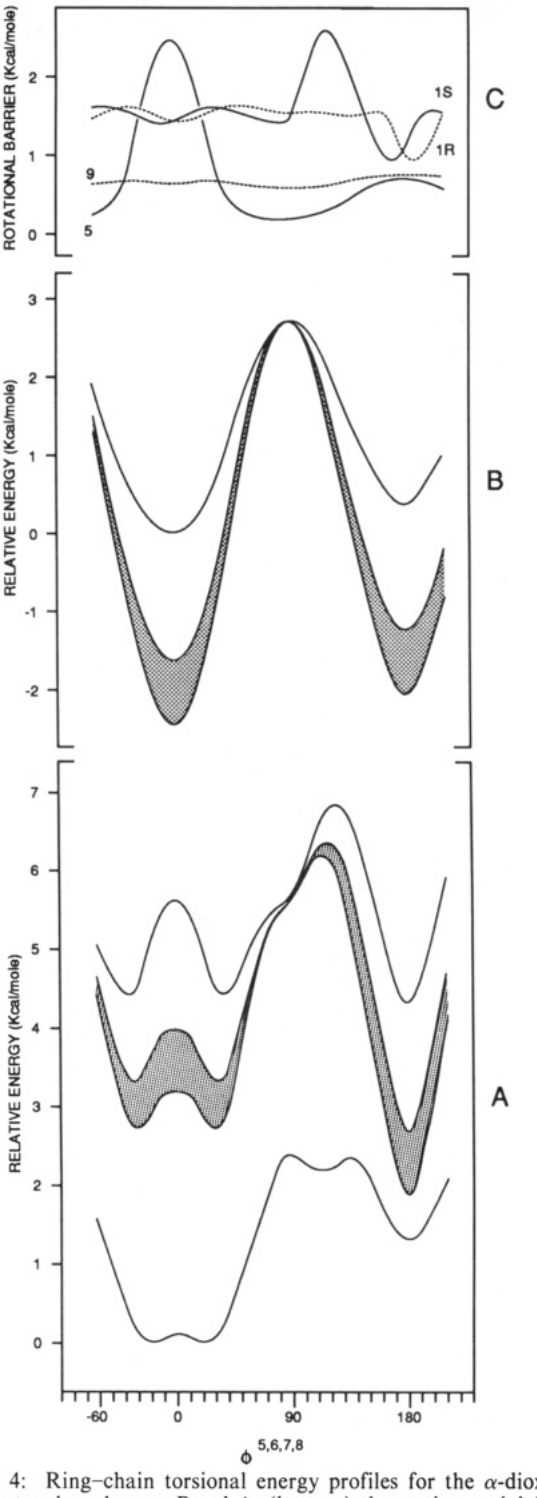

FIGURE 4: Ring–chain torsional energy profiles for the α-dioxocyclopentenyl analogue. Panel A, (bottom) the static quasiglobal minimum energy profile of the full analogue; (top) the dynamic quasiglobal minimum energy profile not corrected for the AM1 underestimate of the C^6–C^7 torsional barrier; (middle, shaded region) the corrected dynamic quasiglobal minimum energy profile. B, (top) the AM1-determined C^6–C^7 torsional barrier for the desmethyl α-dioxocyclopentenyl analogue truncated at C^{10}; (bottom, shaded region) the corrected C^6–C^7 torsional barrier for the desmethyl α-dioxocyclopentenyl analogue. Panel C, the methyl rotational barriers used to correct the static minimum energy profile shown in panel A.

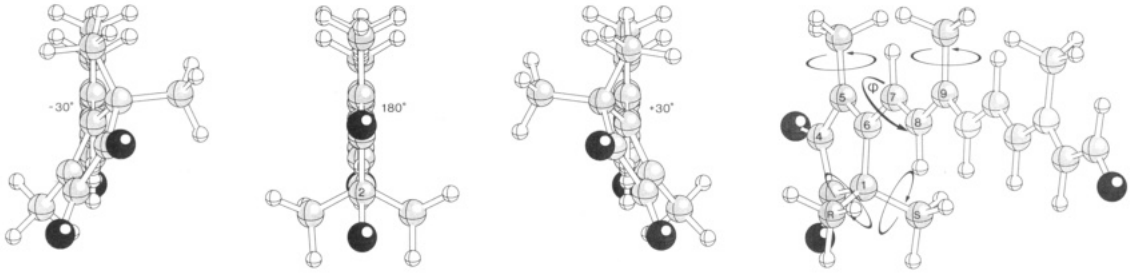

FIGURE 5: Ball-and-stick depictions of the conformations of the ring–polyenal juncture of α-dioxocyclopentenylretinal. (Right) the relative geometries of the methyl protons and 7H and 8H and the rotations of interest; (middle and left) the end-views of the three ring–chain solution conformers.

1 and 7, respectively, in the electron density map of bR (Trewhella et al., 1986; Popot et al., 1989) and the positioning of the retinal chromophore within the helix bundle (Seiff et al., 1985; Seiff et al., 1986a; Heyn et al., 1988; Hauss et al., 1990), both having been determined by neutron diffraction analyses of selectively deuterated bR. In addition, the proposed model accommodates readily those structural features essential for a plausible description of the proton-pumping mechanism, which has emerged primarily from functional characterizations of numerous bR mutants by Khorana and co-workers. From this model one would predict that a semiselective arginine modifier such as the α-dioxocyclopentenyl analogue might react with and thereby cross-link to Arg^{134} or Lys^{129}—the only nucleophilic residues near the extracellular interface at the ring end of the retinal-binding site.

This model, however, does not accommodate adequately several structural features in bR determined experimentally or demonstrated theoretically, including (i) the positioning of charged residues within the chromophore binding site as predicted by external point charge contributions to the opsin shift, (ii) the location of Lys^{41} on the electron density map of the helix bundle (Seiff et al., 1986b), and (iii) the unexpectedly straight conformation of helix 7, assigned to putative helix B by Popot et al. (1989). The external point charge contributions to the opsin shift have been dismissed by some, following the biophysical characterization of bR mutants in which native charged residues on the putative transmembrane segments were eliminated or altered (Mogi et al., 1988; Stern & Khorana, 1989). In particular, the relative insensitivity of bR's λ_{max} to the removal of charge from Asp^{212}, the most likely Schiff base counterion, by its mutation to asparagine was interpreted as Asp^{212}'s insignificant contribution to—and, in general, the failure of—the external point charge description of the opsin shift. The significant red shift in λ_{max} accompanying the $Asp^{212} \rightarrow$ Glu mutation was similarly cited as disproof of the external point charge mechanism, a significant blue shift having been anticipated (Mogi et al., 1988). Consequently, this interpretation does not require the explicit positioning of an ion pair near the ring end of the chromophore as demanded by the external point charge mechanism (Honig et al., 1976; Nakanishi et al., 1980; Harbison et al., 1985); accordingly, in the model of Henderson et al. (1990) there is no ion pair near the chromophore's ring, although neither the role of "permanently protonated" Asp^{115} nearby nor the importance of bound metal have yet been evaluated.

There is, however, a plausible interpretation of the spectral properties of bR mutants—including $Asp^{212} \rightarrow$ Asn/Glu—consistent with the external point charge model: counterion stabilization of the protonated Schiff base is likely mediated by a neutral molecule, such as water, this inclusion being accommodated by the relatively large separation (3.5–4.0 Å) of charge centers (Spudich et al., 1986; de Groot et al., 1989); neutralizing the negative charge at Asp^{212} would generate an unpaired ion at the protonated Schiff base, which, in aqueous medium, would likely be countered by buffer electrolytes such as phosphate anion, the net effect on λ_{max} being subtle and dependent upon the difference in the average charge separation as compared to native bR. Given the observed slight decrease in the λ_{max} of light-adapted Asn^{212}-bR, this counterion separation is probably less than 3.9 Å, assuming the phosphate anion is singly charged, a hypothesis testable by determining λ_{max} in buffers containing anions smaller or larger than $H_2PO_4^-$ (Honig et al., 1976). The pronounced red shift in λ_{max} observed for Glu^{212}-bR may be accounted for by assuming that extension of the charged side chain of residue 212 by ≈2.5 Å is accommodated by conformational changes in bR induced either exclusively at the Schiff base end or throughout the binding site as propagated by retinal itself, the net result being that the charge separation at the Schiff base end has *increased* and/or retinal has been forced *nearer* the anionic center of the putative ion pair at the ring end.

Therefore, in order primarily to accommodate the postulated external point charge mechanism for the opsin shift in bR, an alternative to the model of Henderson et al. (1990) was constructed (Figure 6). The chromophore binding site of bR was modeled initially by constructing seven free-standing α-helices having ideal main-chain conformations and random side-chain conformations. To the ε-NH_2 of Lys^{216} on helix G (residues 202–225) was bonded the α-dioxocyclopentenyl analogue of *all-trans*-retinal via an aldimine linkage. To mimic the average tilt of the helices within the bundle (Henderson & Unwin, 1975; Hayward & Stroud, 1981), helix G was tilted slightly (10°) away from the norm of the membrane surface. The side chains of Asp^{212} and Lys^{216} were then manipulated in order to satisfy four criteria: (1) that the distance between the center of charge on the side-chain carboxyl of Asp^{212} and the ε-N of Lys^{216} measured 3.5–4.0 Å (Spudich et al., 1986; de Groot et al., 1989); (2) that the N→H bond vector of the protonated Schiff base was oriented toward the charged side-chain carboxyl of Asp^{212} (Lin & Mathies, 1989); (3) that the plane of the polyene system was oriented perpendicular to the plane of the membrane (Earnest et al., 1986); and (4) that the long axis of the polyene system was inclined 20–25° relative to the plane of the membrane, the ring end being closer to the exterior membrane surface (Ebrey et al., 1977; Heyn et al., 1977; Bogomolni et al., 1980; Hauss et al., 1990). Helices F (residues 174–198), E (residues 133–157), D (residues 107–130), C (residues 79–101), B (residues 41–65), and A (residues 8–31) were then packed in clockwise sequence around the chromophore (as viewed from the membrane's exterior) in order to produce the helix bundle (Henderson & Unwin, 1975; Henderson et al., 1990). Each helix was then rotated about its long axis to mimic their putative inside-out nature, hydrophobes facing predominantly away from the core of the bundle. Helix F was further constrained by rotating it about its long axis to bring Trp^{182}, Tyr^{185}, and Trp^{189} close to the

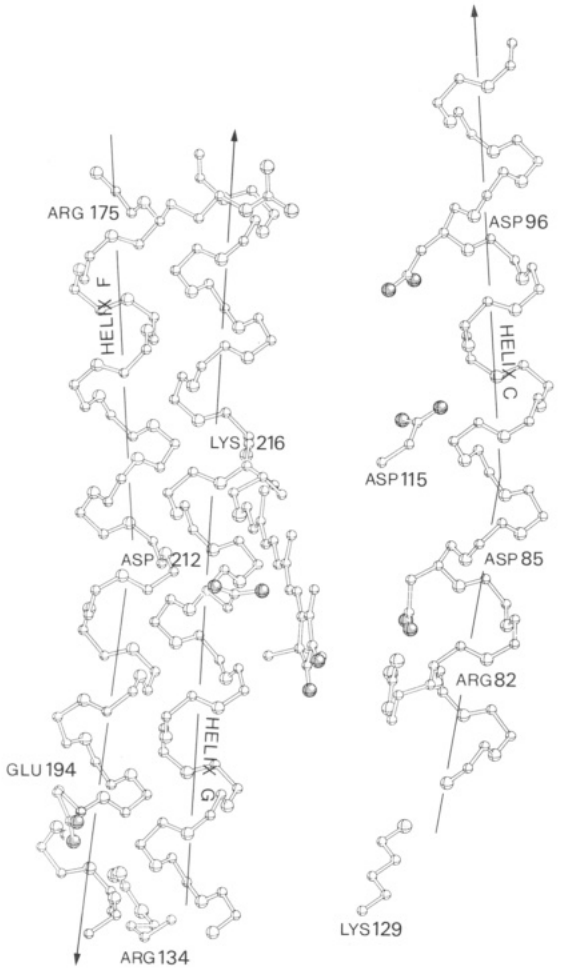

FIGURE 6: Ball-and-stick depiction of an alternate model for the bR helix bundle. Shown are the main-chain atoms of putative helices G, F, and C, the α-dioxocyclopentenyl analogue of retinal, and all charged residues within the bundle. Note the ion pairing of Asp^{85} with Arg^{82}, Glu^{194} with Arg^{134}, and Asp^{212} with the chromophore's protonated Schiff base and the positions of the three arginines relative to the chromophore's ring.

chromophore (Hackett et al., 1987). In addition, helix D was oriented to depict the putative proximity of Thr^{121} and Gly^{122} to the ring end of the chromophore (Ding et al., 1990). Helix–helix contacts within the bundle were no closer than 10Å as measured from helix center to helix center in cross sections of the bundle at both membrane interfaces. Construction of the bR helix bundle in this fashion led naturally to one of the two suggested helix assignments (i.e., 1234567 = *****BA) made on the basis of neutron diffraction results of bR renatured with helices A and B deuterated exclusively (Trewhella et al., 1986), although, on the basis of a more limited deuterium labeling scheme, Popot et al. (1989) concluded that the alternate helix assignment was correct (ie., 1234567 = A*****B). Because 30–40 lipid molecules are believed to encircle each bR trimer in its native environs, a partial collar of lipid bilayer one molecule thick consisting solely of the dihydrophytolphosphatide was placed around the helix bundle from putative helix C to helix G, gauging the depth of the chromophore at near midlevel (Kates et al., 1965; Stoeckenius & Kunau, 1968; Blaurock & Stoeckenius, 1971).

From the bR helix bundle so modeled, several features concerning the placement of charged residues within the chromophore-binding site may be observed (Figure 6): (a) the three arginine residues in halorhodopsin resistant to diphenylglyoxal modification presumably due to their inaccessibility (Ariki et al., 1986) are probably Arg^{82}, Arg^{134}, and Arg^{175}, conserved in bR, as has been suggested (Lanyi et al., 1988); (b) Arg^{82} and Asp^{85} are capable of ion pairing, as has also been suggested (Lanyi et al., 1988) and may be the charge pair postulated to exist near the ring of the chromophore (Harbison et al., 1985; Spudich et al., 1986); (c) Glu^{194} labeled by the photosensitive analogue *m*-diazirinophenylretinal (Huang et al., 1982) is not near the ring of the chromophore; (d) Arg^{134} is within bonding distance of Glu^{194}, these residues possibly forming an interhelical ion-pair; (e) contrary to earlier suggestions (Lanyi et al., 1988), Arg^{175} and Asp^{115} are, in all likelihood, too distant from each other to form an ion pair; and (f) a pair of acidic residues on adjacent helices—Asp^{96} on helix C and Asp^{115} on helix D—are located in the cytoplasmic half of the helix bundle and are sufficiently close to each other (5–7 Å) to chelate between them one of two divalent metal ions putatively tightly bound by purple membrane (Ariki & Lanyi, 1986).

In this alternate model of the bR helix bundle, both charges of the putative Asp^{85}–Arg^{82} ion pair have been positioned 3–4 Å above the face of the retinal ring according to the external point charge model of Spudich et al. (1986), in fair agreement with the placement of charged residues as deduced by Harbison et al. (1985) and indicating that Arg^{82} rather than Arg^{134} would be selectively cross-linked by the α-dioxocyclopentenyl analogue. However, in order to reconcile the pronounced red shift in the λ_{max} for the $Asp^{85} \rightarrow Asn$ mutant of bR (Mogi et al., 1988), one needs to introduce an anion, such as buffer phosphate, into the ring end of the chromophore pocket to counter the buried Arg^{82}. Unlike the protonated Schiff base end that requires increased charge separation to induce a red shift in λ_{max}, the red-shifted λ_{max} of Asn^{85}-bR indicates a closer approach (by less than 1 Å) of the anionic charge center to the ring end of retinal (Honig et al., 1976). Similar steric adjustments may characterize the $Asp^{85} \rightarrow Glu$ mutant as evidenced by the pronounced red shift in λ_{max} for the solubilized form of this bR (Mogi et al., 1988). The pronounced red shift in the λ_{max} for the $Arg^{82} \rightarrow Gln$ mutant (Stern & Khorana, 1989) may also be accounted for by a slight (less than 1 Å) change in the position of Asp^{85} relative to the retinal ring accompanying the introduction of a buffer cation such as Na^+ to counter its charge.

In addition to the opportune placement of an ion pair near the chromophore's ring, this alternate model of the bR helix bundle is consistent both with the localization of Lys^{41} on the projection map of bR (Seiff et al., 1986b) and the apparently unbent conformation of helix 7, assigned here to helix A, which is devoid of proline.

Conclusions

In an attempt to synthesize potential chemical cross-links suitable for studying the chromophore site of retinal-binding proteins, we have made several ring-oxidized *all-trans*-retinals. One of these, the α-dioxocyclopentenyl analogue, exists predominantly as the 6-s-trans conformer and possesses the reactive α-diketo function common to a variety of chemical reagents utilized routinely to modify selectively the nucleophilic guanidinium function of arginyl residues (Means & Feeney, 1971; Riordan, 1979; Gripon & Hofmann, 1981). According to one current description of the chromophore cavity of bR, an ion pair is located at the ring end portion of the retinal binding pocket (Harbison et al., 1985; Spudich et al., 1986). Harbison et al. (1985) have suggested that the cationic component of this pair of postulated point charges may be arginine; Lanyi et al. (1988) have further suggested that the ion pair is Asp^{115}–Arg^{175}. On the basis of the model of Henderson et

al. (1990), which does not explicitly position an ion pair near the ring, Arg^{134} is the residue most likely cross-linked by the α-dioxocyclopentenyl analogue. However, on the basis of our model of the helix bundle built explicitly to accommodate potential external point charge interactions, we suggest that the α-dioxocyclopentenyl analogue bound to the chromophore cavity by its Schiff base linkage at the tail end may be well-positioned to modify Arg^{82} at the ring end via a similar Schiff base like condensation. In support of this suggestion, Beischel et al. (1990; C. Beischel, V. Mani, R. Govindgee, T. G. Ebrey, D. R. Knapp, and R. K. Crouch, to be published) have determined that the α-dioxocyclopentenyl analogue forms pigment as quickly as does native *all-trans*-retinal and that the pigment so formed is incapable of dark-adapting after exposure to white light. In analogy to the use of cyclohexanedione, the α-dihydroxy derivative of the α-dioxo analogue potentially generated by the condensation with an arginine may be stabilized either by borate or acetic acid in order to protect the ring–helix attachment during proteolytic digestions of cross-linked bR (Patthy & Smith, 1975a,b; Austen & Smith, 1976). Alternatively, dehydration of the α-dihydroxy adduct may form the osazone, which, also like the tail-end Schiff base, may be reduced by reagents such as $NaCNBH_3$ to form a cross-link stable toward proteolytic or chemical hydrolysis. Although it should be noted that there is some tendency for α-dicarbonyls to similarly modify lysines, forming oxazoles as end products (Sleath et al., 1985; Rodriquez & Bruice, 1989), Lys^{129} at the head of helix D does not appear in our model or that of Henderson et al. (1990) to be near enough the ring end of the chromophore to cross-link retinal even with its side chain extended fully into the cavity.

Acknowledgments

We thank C. Harvey and T. O'Brien (Department of Pharmacology) for helping to maintain the NMR spectrometer, C. Beischel (Department of Pharmacology) for assistance obtaining mass spectral data and plotting the UV–visible spectra shown in Figure 3, J. Walker (Department of Pharmacology) for assistance recording the FTIR spectra, R. H. Gadsden, Jr. (CSX Academic Systems manager), for his help archiving the AM1 output files and for access to the CSX terminal suite, E. Rivera and P. Ellis (Department of Chemistry, University of South Carolina, Columbia), and W. C. Wise (Department of Physiology) for assistance in coordinate file transfers enabling the use of the program Ball & Stick II (N. Mueller and A. Falk, Linz, Austria) and the construction of Figures 5 and 6, R. Means and C. Batts (Palmetto Repro Graphics, North Charleston, SC) for their expert preparation of the separation negatives used for Figures 1–6, R. P. Thompson and D. R. Di Bona (Department of Anatomy) for access to the E&S Graphics Workstation during the revision of this manuscript, and E. S. Hazard (Department of Ophthalmology), C. Beischel, and R. K. Crouch (Department of Ophthalmology) for critiquing the manuscript. V.M. also acknowledges support by R. K. Crouch through a National Institutes of Health grant (EY-03959).

Supplementary Material Available

A table of atomic Cartesian coordinates for the AM1 geometry-optimized structures of α-dioxocyclopentenylretinal corresponding to the minima in its dynamic energy profile, that is, twisted 6-s-cis ($\phi^{5678} = 30°$) and planar 6-s-trans ($\phi^{5678} = 180°$), a figure showing the long-range scalar interactions in the 2QF-COSY spectrum of 4-oxoretinal, and a figure showing ^{13}C–^{1}H chemical shift correlations and expansions from the ^{1}H-coupled ^{13}C NMR spectrum of 4-oxoretinal (3 pages). Ordering information is given on any current masthead page.

Registry No. 1, 33532-44-4; 2, 131864-85-2; 3, 131903-83-8; retinal, 116-31-4.

References

Allinger, N. L., & Tai, J. C. (1965) *J. Am. Chem. Soc. 87*, 2081–2087.
Ariki, M., & Lanyi, J. (1986) *J. Biol. Chem. 261*, 8167–8174.
Ariki, M., Schobert, B., & Lanyi, J. (1986) *Arch. Biochem. Biophys. 248*, 532–539.
Asato, A. E., Zhang, B.-W., Denny, M., Mirzadegan, T., Seff, K., & Liu, R. S. H. (1989) *Bioorg. Chem. 17*, 410–421.
Aue, W. P., Bartholdi, E., & Ernst, R. R. (1976) *J. Chem. Phys. 64*, 2229–2246.
Austen, B. M., & Smith, E. L. (1976) *J. Biol. Chem. 251*, 5835–5837.
Bachmann, P., Aue, W. P., Müller, L., & Ernst, R. R. (1977) *J. Magn. Reson. 28*, 29.
Balogh-Nair, V., & Nakanishi, K. (1982) *Methods Enzymol. 88*, 496–506.
Balogh-Nair, V., Carriker, J. D., Honig, B., Kamat, V., Motto, M. G., Nakanishi, K., Sen, R., Sheves, M., Arnaboldi Tanis, M., & Tsujimoto, K. (1981) *Photochem. Photobiol. 33*, 483–488.
Barfield, M., & Chakrabarti, B. (1969) *Chem. Rev. 69*, 757–778.
Bart, J. C. J., & MacGillavry, C. H. (1968) *Acta Crystallogr. B24*, 1587.
Baselt, D. R., Fodor, S. P. A., van der Steen, R., Lugtenburg, J., Bogomolni, R. A., & Mathies, R. A. (1989) *Biophys. J. 55*, 193–196.
Bax, A., & Morris, G. (1981) *J. Magn. Reson. 42*, 501–505.
Becker, R. S., Berger, S., Dalling, D. K., Grant, D. M., & Pugmire, R. J. (1974) *J. Am. Chem. Soc. 96*, 7008–7016.
Beischel, C., Mani, V., Williams, T. C., & Crouch, R. K. (1990) *Biophys. J. 57*, 360a.
Blaurock, A. E., & Stoeckenius, W. (1971) *Nature (New Biol.) 233*, 152–155.
Bock, C. W., George, P., Trachtman, M., & Zanger, M. (1979) *J. Chem. Soc., Perkin Trans. 2*, 26–34.
Bogomolni, R. A., Baker, R. A., Lozier, R. H., & Stoeckenius, W. (1980) *Biochemistry 19*, 2152–2159.
Cheney, B. V. (1968) *J. Am. Chem. Soc. 90*, 5386–5390.
Cheney, B. V., & Grant, D. M. (1967) *J. Am. Chem. Soc. 89*, 5319–5327.
Crouch, R. (1986) *Photochem. Photobiol. 44*, 803–807.
de Groot, H. J. M., Harbison, G. S., Herzfeld, J., & Griffin, R. G. (1989) *Biochemistry 28*, 3346–3353.
Dewar, M. J. S., Zoebisch, E. G., Healy, E. F., & Stewart, J. J. P. (1985) *J. Am. Chem. Soc. 107*, 3902–3909.
Ding, W.-D., Tsipouras, A., Ok, H., Yamamoto, T., Gawinowicz, M. A., & Nakanishi, K. (1990) *Biochemistry 29*, 4898–4912.
Earnest, T. M., Roepe, P., Braiman, M. S., Gillespie, J., & Rothschild, K. J. (1986) *Biochemistry 25*, 7793–7798.
Ebrey, T. G., Becher, B., Mao, B., Kilbridge, P., & Honig, B. (1977) *J. Mol. Biol. 130*, 395–404.
Fatiadi, A. J. (1976) *Synthesis 2*, 133–167.
Fatiadi, A. J. (1986) in *Organic Syntheses by Oxidation with Metal Compounds* (Mijs, W. J., & DeJonge, C. R. H. I., Eds.) pp 119–260, Plenum, New York.
Fieser, L. F., & Fieser, M. (1959) *Steroids*, pp 15–25, Reinhold Publishing Corp., New York.
Gieren, A., Lamm, V., Oesterhelt, D., & Schlude, H.-J. (1982) *Z. Naturforsch. 37b*, 1612–1622.

Gilardi, R., Karle, I. L., Karle, J., & Sperling, W. (1971) *Nature 232*, 187–189.

Grant, D. M., & Cheney, B. V. (1967) *J. Am. Chem. Soc. 89*, 5315–5318.

Gripon, J.-C., & Hofmann, T. (1981) *Biochem. J. 193*, 55–65.

Hackett, N. R., Stern, L. J., Chao, B. H., Kronis, K. A., & Khorana, H. G. (1987) *J. Biol. Chem. 262*, 9277–9284.

Hamanaka, T., Mitsui, T., Ashida, T., & Kakudo, M. (1972) *Acta Crystallogr., Sect. B 28*, 214.

Harbison, G. S., Smith, S. O., Pardoen, J. A., Courtin, J. M. L., Lugtenburg, J., Herzfeld, J., Mathies, R. A., & Griffin, R. G. (1985) *Biochemistry 24*, 6955–6962.

Hauss, T., Grzesiek, S., Otto, H., Westerhausen, J., & Heyn, M. P. (1990) *Biochemistry 29*, 4904–4913.

Hayward, S., & Stroud, R. M. (1981) *J. Mol. Biol. 151*, 491–517.

Henbest, H. B., Jones, E. R. H., & Owen, T. C. (1957) *J. Biol. Chem. 47*, 4909–4912.

Henderson, R., & Unwin, P. N. T. (1975) *Nature 257*, 28–32.

Henderson, R., Baldwin, J. M., Ceska, T. A., Zemlin, F., Beckmann, E., & Downing, K. H. (1990) *J. Mol. Biol. 213*, 899–929.

Heyn, M. P., Cherry, R. J., & Mueller, U. (1977) *J. Mol. Biol. 117*, 607–620.

Heyn, M. P., Westerhausen, J., Wallat, I., & Seiff, F. (1988) *Proc. Natl. Acad. Sci. U.S.A. 85*, 2146–2150.

Holzel, R., Leftwick, A. P., & Weedon, B. C. L. (1969) *J. Chem. Soc., Chem. Commun.*, 128.

Honig, B., Hudson, B., Sykes, B. D., & Karplus, M. (1971) *Proc. Natl. Acad. Sci. U.S.A. 68*, 1289–1293.

Honig, B., Warshel, A., & Karplus, M. (1975) *Acc. Chem. Res. 8*, 92–100.

Honig, B., Greenberg, A. D., Dinur, U., & Ebrey, T. G. (1976) *Biochemistry 15*, 4593–4599.

Honig, B., Dinur, U., Birge, R. R., & Ebrey, T. G. (1980) *J. Am. Chem. Soc. 102*, 488–494.

Huang, K.-S., Radhakrishnan, R., Bayley, H., & Khorana, H. G. (1982) *J. Biol. Chem. 257*, 13616–13623.

Jeener, J., Meier, B. H., Bachmann, P., & Ernst, R. R. (1979) *J. Chem. Phys. 71*, 4546–4553.

Karplus, M. (1960) *J. Chem. Phys. 33*, 1842–1849.

Kates, M., Yengoyan, L. S., & Sastry, P. S. (1965) *Biochim. Biophys. Acta 98*, 252–268.

Kollenz, G., & Akcamur, Y. (1984) *Chim. Acta Turc. 12*, 203–215.

Kumar, A., Ernst, R. R., & Wuthrich, K. (1980) *Biochem. Biophys. Res. Commun. 95*, 1–6.

Lanyi, J. K., Zimanyi, L., Nakanishi, K., Derguini, F., Okabe, M., & Honig, B. (1988) *Biophys. J. 53*, 185–191.

Lin, S. W., & Mathies, R. A. (1989) *Biophys. J. 56*, 653–660.

Liu, R. S. H., & Mirzadegan, T. (1988) *J. Am. Chem. Soc. 110*, 8617–8623.

Loncharich, R. J., Schwartz, T. R., & Houk, K. N. (1987) *J. Am. Chem. Soc. 109*, 14–23.

Macura, C., Huang, Y., Suter, D., & Ernst, R. R. (1981) *J. Magn. Reson. 43*, 259–281.

Martin, H.-D., Kummer, M., Martin, G., Bartsch, J., Bruck, D., Heinrichs, A., Mayer, B., Rover, S., Steigel, A., Mootz, D., Middelhauve, B., & Scheutzow, D. (1987) *Chem. Ber. 120*, 1133–1149.

Means, G. E., & Feeney, R. E. (1971) in *Chemical Modification of Proteins*, pp 194–211, Holden-Day, Inc., San Francisco, CA.

Mogi, T., Stern, L. J., Marti, T., Chao, B. H., & Khorana, H. G. (1988) *Proc. Natl. Acad. Sci. U.S.A. 85*, 4148–4152.

Mueller, L., & Ernst, R. R. (1979) *Mol. Phys. 38*, 963–992.

Nakanishi, K., Balogh-Nair, V., Arnaboldi, M., Tsujimoto, K., & Honig, B. (1980) *J. Am. Chem. Soc. 102*, 7945–7947.

Noggle, J. H., & Schirmer, R. E. (1971) *The Nuclear Overhauser Effect: Chemical Applications*, Chapter 3, Academic Press, Inc., New York.

Pasto, D. J., & Johnson, C. R. (1969) *Organic Structure Determination*, p 96, Prentice-Hall, Inc., Englewood Cliffs, NJ.

Patel, D. J. (1969) *Nature 221*, 825–828.

Patthy, L., & Smith, E. L. (1975a) *J. Biol. Chem. 250*, 557–564.

Patthy, L., & Smith, E. L. (1975b) *J. Biol. Chem. 250*, 565–569.

Piantini, U., Sorenson, O. W., & Ernst, R. R. (1982) *J. Am. Chem. Soc. 104*, 6800–6801.

Popot, J.-L., Engelman, D. M., Gurel, O., & Zaccai, G. (1989) *J. Mol. Biol. 210*, 829–847.

Pullman, B., Langlet, J., & Berthod, H. (1969) *J. Theor. Biol. 23*, 482.

Rance, M., Sorensen, O. W., Bodenhausen, G., Wagner, G., Ernst, R. R., & Wuthrich, K. (1983) *Biochem. Biophys. Res. Commun. 117*, 479–485.

Riordan, J. F. (1979) *Mol. Cell. Biochem. 26*, 71–92.

Robeson, C. D., Blum, W. P., Dieterle, J. M., Cawley, J. D., & Baxter, J. G. (1955) *J. Am. Chem. Soc. 77*, 4120–4125.

Rodriquez, E. J., & Bruice, T. C. (1989) *J. Am. Chem. Soc. 111*, 7947–7956.

Rowan, R., III, & Sykes, B. D. (1974) *J. Am. Chem. Soc. 96*, 7000–7008.

Rowan, R., III, & Sykes, B. D. (1975) *J. Am. Chem. Soc. 97*, 1023–1027.

Rowan, R., III, Warshel, A., Sykes, B. D., & Karplus, M. (1974) *Biochemistry 13*, 970–981.

Schenk, H. (1971) *Acta Crystallogr. B27*, 667–672.

Scott, A. I. (1964) *Interpretation of the Ultraviolet Spectra of Natural Products*, pp 45–88, Pergamon Press, Oxford, England.

Sen, R., Carriker, J. D., Balogh-Nair, V., & Nakanishi, K. (1982) *J. Am. Chem. Soc. 104*, 3214–3216.

Seiff, F., Wallat, I., Erman, P., & Heyn, M. P. (1985) *Proc. Natl. Acad. Sci. U.S.A. 83*, 3227–3231.

Seiff, F., Westerhausen, J., Wallat, I., & Heyn, M. P. (1986a) *Proc. Natl. Acad. Sci. U.S.A. 83*, 7746–7750.

Seiff, F., Wallat, I., Westerhausen, J., & Heyn, M. P. (1986b) *Biophys. J. 50*, 629–635.

Shaka, A. J., Keeler, J., & Freeman, R. (1983) *J. Magn. Reson. 53*, 313–340.

Simmons, C. J., Asato, A. E., & Liu, R. S. H. (1986a) *Acta Crystallogr. C42*, 711–715.

Simmons, C. J., Asato, A. E., Denny, M., & Liu, R. S. H. (1986b) *Acta Crystallogr. C42*, 1558–1563.

Sleath, P. R., Noar, J. B., Eberlein, G. A., & Bruice, T. C. (1985) *J. Am. Chem. Soc. 107*, 3328–3338.

Sokolova, N. A., Mitsner, B. I., & Zakis, V. I. (1979) *Bioorg. Khim. 5*, 1053–1058.

Spudich, J. L., McCain, D. A., Nakanishi, K., Okabe, M., Shimizu, N., Rodman, H., Honig, B., & Bogomolni, R. A. (1986) *Biophys. J. 49*, 479–483.

Squillacote, M. E., Sheridan, R. S., Chapman, O. L., & Anet, F. A. L. (1979) *J. Am. Chem. Soc. 101*, 3657–3659.
States, D. J., Haberkorn, R. A., & Reuben, D. J. (1982) *J. Magn. Reson. 48*, 286–282.
Stern, L. J., & Khorana, H. G. (1989) *J. Biol. Chem. 264*, 14202–14208.
Stoeckenius, W., & Kunau, W. H. (1968) *J. Cell Biol. 38*, 337–357.
Trewhella, J., Popot, J.-L., Zaccai, G., & Engelman, D. (1986) *EMBO J. 5*, 3045–3049.
van der Steen, R., Biesheuvel, P. L., Mathies, R. A., & Lugtenburg, J. (1986) *J. Am. Chem. Soc. 108*, 6410–6411.
Warshel, A., & Karplus, M. (1974) *J. Am. Chem. Soc. 96*, 5677–5689.
Wernly, J., & Lauterwein, J. (1983) *Helv. Chim. Acta 66*, 1576–1587.
Woodward, R. B. (1941) *J. Am. Chem. Soc. 63*, 1123–1126.
Woodward, R. B. (1942a) *J. Am. Chem. Soc. 64*, 72–75.
Woodward, R. B. (1942b) *J. Am. Chem. Soc. 64*, 76–77.

CORRECTIONS

Structural Description of Acid-Denatured Cytochrome *c* by Hydrogen Exchange and 2D NMR, by Mei-Fen Jeng, S. Walter Englander, Gülnur Elöve, A. Joshua Wand, and Heinrich Roder*, Volume 29, Number 46, November 20, 1990, pages 10433–10437.

Page 10436. The equation in the legend to Figure 2 should read

$$\epsilon(\mathrm{pH}) = \epsilon_N + (\epsilon_A - \epsilon_N)/[1 + 10^{n(\mathrm{pH}-\mathrm{p}K_1)}] + (\epsilon_U - \epsilon_A)/[1 + 10^{n(\mathrm{pH}-\mathrm{p}K_2)}]$$

Asymmetric Structure of a Three-Arm DNA Junction, by Qiu Guo, Min Lu, M. E. A. Churchill, T. D. Tullius, and N. R. Kallenbach*, Volume 29, Number 49, December 11, 1990, pages 10927–10934.

Pages 10929 and 10930. Figures 3 and 4 are reversed. The captions are correct as printed.